Magnetic Modules

DOI: 10.1002/ange.201309981

$[ReF_6]^{2-}$: A Robust Module for the Design of Molecule-Based Magnetic Materials**

Kasper S. Pedersen, Marc Sigrist, Mikkel A. Sørensen, Anne-Laure Barra, Thomas Weyhermüller, Stergios Piligkos, Christian Aa. Thuesen, Morten G. Vinum, Hannu Mutka, Høgni Weihe, Rodolphe Clérac,* and Jesper Bendix**

Abstract: *A facile synthesis of the $[ReF_6]^{2-}$ ion and its use as a building block to synthesize magnetic systems are reported. Using dc and ac magnetic susceptibility measurements, INS and EPR spectroscopies, the magnetic properties of the isolated $[ReF_6]^{2-}$ unit in $(PPh_4)_2[ReF_6]\cdot 2H_2O$ (**1**) have been fully studied including the slow relaxation of the magnetization observed below ca. 4 K. This slow dynamic is preserved for the one-dimensional coordination polymer $[Zn(viz)_4(ReF_6)]_\infty$ (**2**, viz = 1-vinylimidazole), demonstrating the irrelevance of low symmetry for such magnetization dynamics in systems with easy-plane-type anisotropy. The ability of fluoride to mediate significant exchange interactions is exemplified by the isostructural $[Ni(viz)_4(ReF_6)]_\infty$ (**3**) analogue in which the ferromagnetic Ni^{II}–Re^{IV} interaction ($+10.8\ cm^{-1}$) dwarfs the coupling present in related cyanide-bridged systems. These results reveal $[ReF_6]^{2-}$ to be an unique new module for the design of molecule-based magnetic materials.*

Diffuse orbitals and large magnetic anisotropies resulting from strong spin-orbit coupling make complexes with central ions from the 4d and 5d series interesting modules for magnetic materials.[1] The preponderance of homo-[2] and heteroleptic[3] cyanide building units has been hard to challenge in the field of molecular magnetism and only few exceptions have been reported.[4] Although homoleptic fluoride complexes are well-described in the literature, they have been used only once[5] as modules to design molecule-based magnetic materials. The rarity of hexafluoridometalate-based magnetic materials may be due to the harsh synthetic conditions often required for the formation of fluoridometalates and to their common inherent lability, outside hydrofluoric acid solutions, towards, for example, hydrolysis. The combination of the kinetic inertness of octahedral d^3 complexes and the potential strong magnetic anisotropy of 5d systems, led us to explore the $[ReF_6]^{2-}$ ion as a possible module to build molecule-based magnetic materials. $[ReF_6]^{2-}$ can be generated by dissolving $[ReX_6]^{2-}$ (X = Cl, Br) salts in a KHF_2 melt.[6] The subsequent isolation of water-soluble $K_2[ReF_6]$ from mixtures with KF and KHF_2 is however problematic. Instead, we found that using molten NH_4HF_2 as a fluoride source, gave quantitatively the water-soluble $(NH_4)_2[ReF_6]$ salt that is easily converted into $(PPh_4)_2[ReF_6]\cdot 2H_2O$ (**1**) by metathesis. The molecular structure of the $[ReF_6]^{2-}$ unit in **1** (hydrogen bonded to two water molecules) is shown in Figure 1 (left) and Figure S1 of the Supporting Information.

When 1-vinylimidazole (viz) is added to a methanol solution of $[ReF_6]^{2-}$ and M^{2+} (M = Zn, Ni), chains with alternating metal centers, $[M(viz)_4(ReF_6)]_\infty$ (M = Zn (**2**), Ni

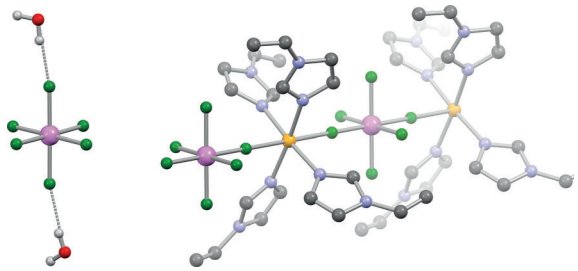

Figure 1. Structures of the $[ReF_6]^{2-}\cdot 2H_2O$ unit in **1** (left) and the chain motif of **2** and **3** (right). Re pink, Zn/Ni yellow, F green, O red, N blue, C gray; H small, light gray. $[PPh_4]^+$ ions and viz hydrogen atoms are omitted for clarity. Selected bond lengths [Å] and angles [°] for **1**: Re-F 1.9515(11)–1.9720(11), **2**: Re-F_{ax} 1.964(3), Re-F_{eq} 1.950(3), Re-F-Zn 180 **3**: Re-F_{ax} 1.9627(16), Re-F_{eq} 1.9496(13); Re-F-Ni 180.

[*] K. S. Pedersen, M. Sigrist, M. A. Sørensen, Dr. S. Piligkos, Dr. C. Aa. Thuesen, M. G. Vinum, Dr. H. Weihe, Prof. Dr. J. Bendix
Department of Chemistry, University of Copenhagen
Universitetsparken 5, 2100 Copenhagen (Denmark)
E-mail: ksp@kiku.dk
bendix@kiku.dk

K. S. Pedersen, Dr. R. Clérac
CNRS, CRPP, UPR 8641
33600 Pessac (France)
and
Univ. Bordeaux, CRPP, UPR 8641
33600 Pessac (France)
E-mail: clerac@crpp-bordeaux.cnrs.fr

M. Sigrist, H. Mutka
Institut Laue-Langevin
38042 Grenoble Cedex 9 (France)

Dr. A.-L. Barra
Laboratoire National des Champs Magnétiques Intenses, CNRS
38042 Grenoble Cedex 9 (France)

Dr. T. Weyhermüller
Max Planck Institute for Chemical Energy Conversion
Mülheim an der Ruhr (Germany)

[**] K.S.P. and S.P. thank the Danish Ministry of Science, Innovation and Higher Education for an EliteForsk travel scholarship and a Sapere Aude Fellowship (10-081659), respectively. This work was partially supported by the University of Bordeaux, the Région Aquitaine, the ANR and the CNRS. J.B. thanks the Danish Research Councils for Independent Research for support (12-125226).

Supporting information for this article is available on the WWW under http://dx.doi.org/10.1002/anie.201309981.

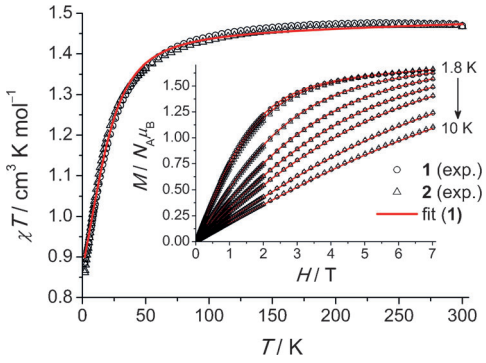

Figure 2. Temperature dependence of the χT product for **1** (circles) and **2** (triangles) at 1000 Oe. Inset: Field dependence of the magnetization between 1.8 and 10 K. The red lines are the best fit for **1** as described in the text.

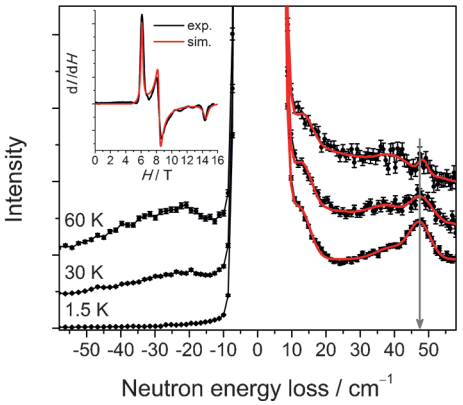

Figure 3. INS spectra of fully deuterated **1** ($\lambda_i = 2.2$ Å, linear momentum (Q) range of 0.80 Å$^{-1} \le Q \le$ 1.65 Å^{-1} at the magnetic peak position). The solid red line represents a sum of four Gaussians. Gray arrow highlights the peaks at 48 cm^{-1}. Inset: HF-EPR spectrum obtained at 5.4 K with 331.2 GHz microwave radiation and its simulation.

(**3**)), are formed. These compounds crystallize in the $P4_2/n$ space group with the Re^{IV} ion occupying a tetragonal position with a slight tetragonal elongation of the octahedron (Figure 1 (right), Figures S2, S3). Despite the different local environments, the magnetism of the isolated Re^{IV} site in the $[PPh_4]^+$ salt, **1**, and the Zn^{II} chain, **2**, are nearly perfectly overlapping as illustrated by the χT versus T ($\chi = M/H$) and M versus H data shown in Figure 2.

The χT product decreases steadily from the room temperature value of 1.43 cm^3 K mol^{-1} to 0.88 cm^3 K mol^{-1} at 1.8 K. As the $[ReF_6]^{2-}$ ions in **1** are separated by more than 11 Å, the main origin for the χT decrease is the single-ion anisotropy (zero-field splitting, ZFS). The magnetic and spectroscopic data for the $S = 3/2$ system were fitted or simulated, respectively, considering the following spin-Hamiltonian Equation (1):

$$\hat{H} = \mu_B g H \hat{S} + D\left(\hat{S}_z^2 - \frac{1}{3}S(S+1)\right) + E\left(\hat{S}_x^2 - \hat{S}_y^2\right) \quad (1)$$

where D and E are the axial and rhombic ZFS parameters, respectively, and the remaining symbols have their usual meaning. To unravel the magnetic anisotropy of **1**, high-field (HF) and X-band EPR spectroscopy and inelastic neutron scattering (INS) were employed. The rough estimation of D from the χT versus T data [Figure 2, Eq. (1)] leads to a value of around 28 cm^{-1} (40 K). The splitting between the two doublets of $2\sqrt{D^2 + 3E^2}$ can be directly probed in zero magnetic field by INS as shown in Figure 3 and Figures S8–S9 for a fully deuterated sample of **1**.

The magnetic origin of the prominent peak observed at 48 cm^{-1} was demonstrated on the basis of its temperature and Q dependence (Figure S9). The combined analysis of HF-EPR (Figure 3) which mainly probes the $|E|/D$ ratio, and INS spectroscopic data allows an accurate evaluation of $g = 1.69$, $D = 23.6$ cm^{-1} (34.0 K), and $|E| = 2.6$ cm^{-1} (3.7 K). Fixing D and E to these spectroscopically determined values, the fitting of the dc magnetic data with only an isotropic g factor leads to $g = 1.76$ and 1.72 for the χT versus T and M versus H data, respectively [red solid lines in Figure 2, Eq. (1)]. The slightly lower g factor for the low-temperature magnetization data is in agreement with the estimation from EPR (Figure 3, Figures S11–S12) and can be explained by different effective g factors of the two doublets resulting from the strong spin-orbit coupling (see Supporting Information). Attempts to spectroscopically measure the zero-field splitting in **2** by INS were unsuccessful, possibly due to the large incoherent cross section of the protons. However, the strong similarity of the magnetic data for **1** and **2** suggests a similar inter-Kramers doublet separation. Using the angular overlap model (AOM) with $e_\sigma^{average} = 13\,000$ cm^{-1} and $e_\pi^{average} = 2000$ cm^{-1} ($\Delta_O = 3e_\sigma - 4e_\pi$) and introducing a small anisotropy between the axial and equatorial fluoride ligands such that $e_{\sigma,ax.} < e_{\sigma,eq.}$ and $e_{\pi,ax.} < e_{\pi,eq.}$ readily accounts for the sign and magnitude of the observed D value (Figure S13–S16).[7]

Despite the positive sign of D, ac susceptibility measurements were performed for **1** and **2**. In zero-dc field, no slow relaxation of the magnetization was observed. However, application of a small dc field gives rise to clear peaks in the out-of-phase component, χ'', of the ac susceptibility (Figures 4 and S19–S26) characteristic of slow dynamics of the magnetization. The associated relaxation times, τ, at the optimum field, H^*, of 2500 Oe (Figures S21, S22, S25, and S26) follow an Arrhenius law, $\tau(T) = \tau_0 \exp\{\Delta_{eff}/(k_B T)\}$, with $\Delta_{eff} = 19.7$ cm^{-1} (28.3 K; $\tau_0 = 9.6 \times 10^{-9}$ s) and $\Delta_{eff} = 20.6$ cm^{-1} (29.6 K; $\tau_0 = 4.7 \times 10^{-10}$ s) for **1** and **2**, respectively (Figure 4). This dynamic behavior parallels that of a few other mononuclear complexes reported to exhibit single-molecule magnet (SMM) properties notwithstanding $D > 0$.[8] Moreover, note that the $[ReF_6]^{2-}$ module is only the second example of a mononuclear 5d complex for which slow relaxation of magnetization has been observed.[9] Intriguingly, the magnetization dynamics of **1** and **2** are strongly similar, indicating that the slow relaxation is not solely a property of the crystal lattice and its heat capacity.[10] Notably, the strictly axial symmetry of **2** precludes a rationalization of the relaxation barrier in terms of rhombicity. The hyperfine couplings in **2** were determined by X-band EPR at $A_z =$

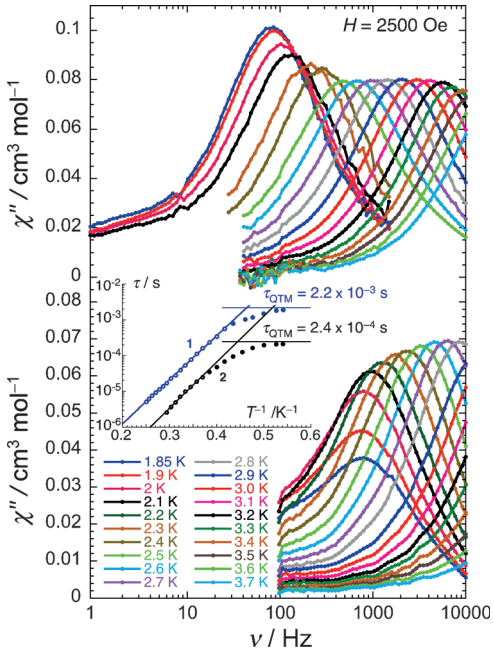

Figure 4. Frequency dependence of the out-of-phase component (χ'') of the ac susceptibility for **1** (top) and **2** (bottom) at selected temperatures between 1.85 and 3.7 K in an 2500 Oe dc field. Inset: τ versus $1/T$ plot for **1** and **2**. The data points were extracted from the $\chi''(\nu)$ maxima at 2500 Oe with $\tau = (2\pi\nu_{ac})^{-1}$.The solid lines corresponds to the fit of the data to an Arrhenius law (see text).

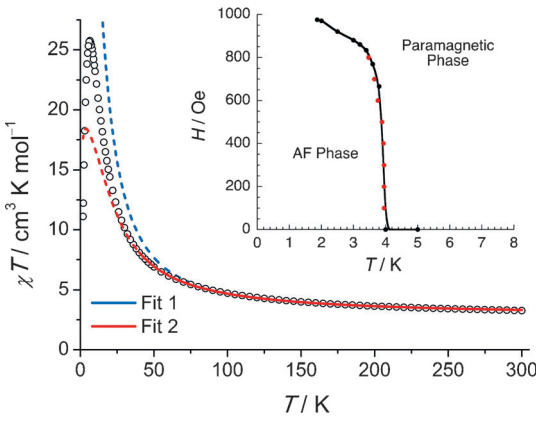

Figure 5. Temperature dependence of the χT product for **3** at 1000 Oe. The solid blue and red lines represent fit 1 and fit 2, respectively, as described in the text. The dashed lines are the extrapolation of the fits to 1.8 K. Inset: (T, H) magnetic phase diagram for **3** extracted from the dM/dH versus H maxima (black points) and χ versus T data at low fields (red points; Figures S28, S29).

0.06179(7) cm^{-1} and $A_{xy} = 0.04953(1)$ cm^{-1} studying the diamagnetic isomorphous $[Zn(viz)_4(ZrF_6)]_\infty$ analogue doped with Re^{IV} (ca. 5%; Figure S12). Interestingly, the associated energy of $A_z S_{Re} I_{Re} \approx 0.23$ cm^{-1} ($I(^{185,187}Re) = 5/2$) is close to the magnetic energy, 0.3 cm^{-1} ($g_{Re}\mu_B H^* S_{Re}$) at the optimum field (2500 Oe) in the ac measurements. In conjunction with the similarity of the magnetic properties of **1** and **2** (Figure 2), this observation could suggest that the magnetization dynamics is more influenced by the interaction between electronic and nuclear spins than by the spin-phonon coupling.

Lowering the temperature, the χT product of **3** (Figure 5) is increasing from 3.3 $cm^3 K mol^{-1}$ at 300 K until reaching a maximum of 25.8 $cm^3 K mol^{-1}$ at 6.5 K. This increase suggests intra-chain Re^{IV}–Ni^{II} ferromagnetic interactions, which are readily explained by the strict orthogonality of the respective t_{2g}^3 and $t_{2g}^6 e_g^2$ configurations resulting from the perfectly linear fluoride bridge. The modeling of the magnetic susceptibility was performed using the following Heisenberg chain Hamiltonian [Eq. (2)].

$$\hat{H} = \mu_B H \sum_i g_i \hat{S}_i - 2J \sum_i \hat{S}_i \hat{S}_{i+1} \qquad (2)$$

The high-temperature data, where quantum effects and magnetic anisotropy have less influence,[11] have been modeled by the approach suggested by Drillon et al. for classical spins in the zero-field limit (fit 1, see Supporting Information)[12] and by exact block diagonalization of the spin-Hamiltonian matrix for a twelve-membered $\{Ni^{II}Re^{IV}\}_6$ ring model (fit 2).[13] These magnetic models yield similar large J interactions evaluated at 10.8(8) cm^{-1} (15.5 K, fit 1) and 11.8(5) cm^{-1} (17.0 K, fit 2).

Using the X-ray structure and calculating J by DFT methods (see Supporting Information) yields $J = 12.7$ cm^{-1} (18.3 K) in good agreement with the above models. For Re^{IV}–Ni^{II} linkages, the fluoride-mediated interaction exceeds the strongest interactions observed through for example, cyanide (3.7 cm^{-1}).[3,14,15] In **3**, no slow relaxation of the magnetization was observed by ac technique (even under dc field), but the field-dependence of the low-temperature magnetization exhibits a characteristic S-shape (Figures S27, S28) indicative of an antiferromagnetic ground state below approximately 4 K (see Supporting Information). From the inflection points of M versus H plots and the χ versus T data at low fields, the temperature dependence of the critical field H_C was extracted and shown in the inset of Figure 5. The magnitude of the antiferromagnetic inter-chain interactions (zJ') is also estimated from $g_{av}\mu_B H_C^0 S_{eff} = 2\,|\,zJ'\,|\,S_{eff}^2$, where H_C^0 is the critical field extrapolated to $T = 0$ K and S_{eff} is the effective spin of 5/2, yielding $zJ' \approx -0.018$ cm^{-1} (−0.026 K). It is important to mention that **3** does not exhibit single-chain magnet properties for two main reasons: 1) the local planar anisotropy for rhenium ($D_{Re} > 0$) that is expected to dominate the chain properties, and 2) the strict tetragonal symmetry of the chains that prevents the canting of the anisotropy axes/planes and thus prevents single-chain magnet behavior.

In summary, a new high-yield synthesis of the $[ReF_6]^{2-}$ ion is described and a detailed study of its physical properties reported, revealing its pronounced magnetic anisotropy upon small structural distortions and its intrinsic slow magnetization dynamics. The chemical robustness allowed its use as a module to synthesize one-dimensional coordination polymer with 3d metal ions. Its ability to mediate significantly strong exchange interactions between magnetic metal ions makes $[ReF_6]^{2-}$ an interesting and unique module for the design of new molecule-based magnetic materials.

Experimental Section

$(NH_4)_2[ReCl_6]$ was prepared as described in literature and the synthesis of $(NH_4)_2[ReF_6]$ is described in the Supporting Information.[16] All other reagents were purchased from commercial sources and used as received.

1: A saturated aqueous solution of PPh_4Cl (0.75 g, 2.0 mmol) was added to a saturated aqueous solution of $(NH_4)_2[ReF_6]$ (0.25 g, 0.74 mmol). The mixture was left standing for 12 h to yield $(PPh_4)_2[ReF_6]\cdot 2H_2O$. Yield: 0.43 g (57%). Elemental Analysis (%) calcd for $C_{48}H_{44}F_6O_2P_2Re$: C 56.80, H 4.37, F 11.23; found: C 56.61, H 4.22, F 11.18. The deuterated analogue was synthesized similarly by using $[D_{20}]PPh_4Cl$ in D_2O (see the Supporting Information).

$[M(viz)_4(ReF_6)]_\infty$ (Zn (**2**), Ni (**3**)): $(PPh_4)_2[ReF_6]\cdot 2H_2O$ (100 mg, 0.099 mmol) and $NiCl_2\cdot 6H_2O$ (100 mg, 0.42 mmol) or $Zn(NO_3)_2\cdot 6H_2O$ (125 mg, 0.42 mmol) were dissolved in MeOH (40 mL) before adding 1-vinylimidazole (0.8 g, 8.5 mmol). The solution was left standing for 1 day to give **2** and **3**, respectively. Yields: **2**: 56 mg (76%), **3**: 52 mg (72%). Elemental Analysis (%) calcd for $C_{20}H_{24}F_6N_8ZnRe$ (**2**): C 32.37, H 3.26, N 15.10; found: C 32.65, H 3.13, N 15.05. Elemental Analysis (%) calcd for $C_{20}H_{24}F_6N_8NiRe$ (**3**): C 32.67, H 3.29, N 15.24, F 15.50; found: C 32.69, H 3.20, N 15.20, F 15.36.

Crystallographic data and additional experimental details of the characterization, spectroscopic data, magnetic properties and the DFT calculations can be found in the Supporting Information. CCDC 964856–964859, contain the supplementary crystallographic data for this paper. These data can be obtained free of charge from The Cambridge Crystallographic Data Centre via www.ccdc.cam.ac.uk/data_request/cif.

Received: October 24, 2013
Revised: November 17, 2013

Keywords: coordination polymers · fluoride · magnetic anisotropy · rhenium · single-molecule magnets

[1] X.-Y. Wang, C. Avendano, K. R. Dunbar, *Chem. Soc. Rev.* **2011**, *40*, 3213.
[2] a) D. E. Freedman, D. M. Jenkins, A. T. Iavarone, J. R. Long, *J. Am. Chem. Soc.* **2008**, *130*, 2884; b) K. S. Pedersen, M. Schau-Magnussen, J. Bendix, H. Weihe, A. V. Palii, S. I. Klokishner, S. Ostrovsky, O. S. Reu, H. Mutka, P. L. W. Tregenna-Piggott, *Chem. Eur. J.* **2010**, *16*, 13458; c) K. Qian, X.-C. Huang, C. Zhou, X.-Z. You, X.-Y. Wang, K. R. Dunbar, *J. Am. Chem. Soc.* **2013**, *135*, 13302.
[3] a) T. D. Harris, M. V. Bennett, R. Clérac, J. R. Long, *J. Am. Chem. Soc.* **2010**, *132*, 3980; b) I. Bhowmick, E. A. Hillard, P. Dechambenoit, C. Coulon, T. D. Harris, R. Clérac, *Chem. Commun.* **2012**, *48*, 9717; c) X. Feng, J. Liu, T. D. Harris, S. Hill, J. R. Long, *J. Am. Chem. Soc.* **2012**, *134*, 7521.
[4] J. Martínez-Lillo, D. Armentano, G. De Munno, W. Wernsdorfer, M. Julve, F. Lloret, J. Faus, *J. Am. Chem. Soc.* **2006**, *128*, 14218.
[5] T. Mahenthirarajah, Y. Li, P. Lightfoot, *Inorg. Chem.* **2008**, *47*, 9097.
[6] a) R. D. Peacock, *J. Chem. Soc.* **1956**, 1291; b) E. Weise, *Z. Anorg. Allg. Chem.* **1956**, *283*, 377.
[7] C. K. Jørgensen, K. Schwochau, *Z. Naturforsch. A* **1965**, *20*, 65.
[8] a) J. M. Zadrozny, J. Jui, N. A. Piro, C. J. Chang, S. Hill, J. R. Long, *Chem. Commun.* **2012**, *48*, 3927; b) J. Vallejo, I. Castro, R. Ruiz-García, J. Cano, M. Julve, F. Lloret, G. De Munno, W. Wernsdorfer, E. Pardo, *J. Am. Chem. Soc.* **2012**, *134*, 15704; c) E. Colacio, F. Ruiz, E. Ruiz, E. Cremades, J. Krzystek, S. Carretta, J. Cano, T. Guidi, W. Wernsdorfer, E. K. Brechin, *Angew. Chem. Int. Ed.* **2013**, *52*, 9130; d) W. Huang, T. Liu, D. Wu, J. Cheng, Z. W. Ouyang, C. Duan, *Dalton Trans.* **2013**, *42*, 15326.
[9] J. Martínez-Lillo, T. F. Mastropietro, E. Lhotel, C. Paulsen, J. Cano, G. De Munno, J. Faus, F. Lloret, M. Julve, S. Nellutla, J. Krzystek, *J. Am. Chem. Soc.* **2013**, *135*, 13737.
[10] H. B. G. Casimir, F. K. Du Pré, *Physica V* **1938**, *6*, 507.
[11] For fits 1 and 2, the experimental data were fitted in the 80–300 K and 40–300 K temperature ranges, respectively.
[12] M. Drillon, E. Coronado, D. Beltran, R. Georges, *Chem. Phys.* **1983**, *79*, 449.
[13] T. Birk, K. S. Pedersen, S. Piligkos, C. A. Thuesen, H. Weihe, J. Bendix, *Inorg. Chem.* **2011**, *50*, 5312.
[14] However, a stronger coupling through cyanide was found in a cyanide-based $Cu^{II}-Re^{IV}$ chain ($J=+29\ cm^{-1}$); T. D. Harris, C. Coulon, R. Clérac, J. R. Long, *J. Am. Chem. Soc.* **2011**, *133*, 123.
[15] I. Bhowmick, T. D. Harris, P. Dechambenoit, E. A. Hillard, C. Pichon, I.-R. Jeon, R. Clérac, *Sci. China Chem.* **2012**, *55*, 1004.
[16] G. W. Watt, R. J. Thompson, *Inorg. Synth.* **1963**, *7*, 189.